



## Experimental Study of a Wave Energy Converter Using a Unidirectional Cascaded Gear System in a Short-Wave Period

Rizki Mendung Ariefianto<sup>1\*</sup>, Yoyok Setyo Hadiwidodo<sup>1</sup>, Shade Rahmawati<sup>1</sup>

<sup>1</sup>*Department of Ocean Engineering, Faculty of Marine Technology, Institut Teknologi Sepuluh Nopember, Surabaya 60111, Indonesia*

**Abstract.** A wave energy converter (WEC) based on a direct mechanical drive system (DMDS) exhibits limited performance when the sea state stands for a short period. This study aims to increase the efficiency of a WEC-DMDS mechanical system applied under short-wave conditions. A novel WEC is designed by applying cascaded gear and reducing the flywheel inertia to achieve better efficiency in a short-wave period. By applying a short-wave period of less than 2.84 s for the actual scale, the UCG-WEC can produce a CWR of 18.5%, mechanical efficiency of 87%, and a maximum power of 200 W. These values are much better than those obtained previously, where zero efficiencies were achieved for the same wave period range. In addition, this model performs well under both high-and low-wave steepness conditions. This study also evaluates variations in lever length and effective height. The C-type configuration, with a relative length ratio of 0.74, is found to be the optimal choice.

**Keywords:** Direct mechanical drive system; Efficiency; Short-wave period; UCG-WEC; Wave energy

### 1. Introduction

Among the ocean energy sources, wave energy deserves consideration because of its ability to produce more than 1–10 TW of electrical energy, which can fulfill the daily energy needs of humans (Farrok et al., 2020). The considerable potential and benefits of wave energy have motivated researchers to design various wave energy converter (WEC) models (Chen et al., 2019). Of these, an oscillating buoy WEC is the most well-known model, which can harness the wave and gravitational energies simultaneously (Li et al., 2013). This WEC has attracted considerable attention because of its several merits, such as a relatively simple design (Rahmati & Aggidis, 2017), higher efficiency, and more feasibility along coastline areas with low energy density (Shi et al., 2019).

However, an oscillating buoy WEC has a smaller geometry than the wavelength, which makes the absorption efficiency unfavorable (Falcão, 2010). To harness the benefits while addressing the weakness of this WEC, it has been integrated with a power take-off (PTO) mechanism. Several PTO methods have been proposed to extract wave energy, with the most familiar types being a hydraulic converter and an electrical direct drive system. However, a hydraulic converter often experiences an oil leakage problem, which causes pollution and damage to the marine environment (López et al., 2013). Meanwhile,

\*Corresponding author's email: [cakmendung97@gmail.com](mailto:cakmendung97@gmail.com), Tel. +62-81-228548237

doi: [10.14716/ijtech.v13i2.5071](https://doi.org/10.14716/ijtech.v13i2.5071)

electrical component protection and air gap arrangement are the main drawbacks of electrical direct drive systems (Mueller & Bakker, 2005). Consequently, fabricating a WEC from such systems is not favorable due to the design complexity and production cost. Hence, the employ of mechanical gear or a direct mechanical drives system (DMDS) has been proposed to convert wave energy to the maximum possible extent, with system simplicity, affordable fabrication costs, and ease of repair (Têtu, 2017; Yang et al., 2019).

A WEC-DMDS has been extensively studied. Lok (2010) conducted experiments on a 1:66.7 scaled WEC based on a gear-flywheel system at a wave height of 2.24–4.48 cm, wave period of 0.75–1.45 s, and maximum captured width ratio (CWR) of 60%. Chandrasekaran and Harender (2012) conducted experiments on a rack-chain-gear WEC model using regular waves, considering a device scale of 1:8.8, wave height of 5–30 cm, and wave period of 1–3 s. According to the results, the highest power was achieved at 30 cm wave height and 2.5 s wave period. Chandrasekaran and Raghavi (2015) designed a lever-gear-flywheel WEC scaled at 1:6, which was tested at 24–30 cm wave height and 3 s wave period in a regular wave. The highest efficiency of 23% was achieved using a lever length of 1.7 m. A similar WEC model using a rack-gear-flywheel system was equally carried out by Peng et al. (2015) and Binh et al. (2016), obtaining final efficiencies of 14% and 28.47%, respectively. Another model using a counterweight-multiplying gear system was examined by Han et al. (2015), which yielded an efficiency of up to 47%.

However, all the abovementioned WEC models were mostly tested at wave periods between 7 and 12 s at the prototype scale, which is not affected by local wind seas (Ahn et al., 2019). In contrast, Têtu (2017) found that the main problem of WECs based on the DMDS concept is their performance limitation when the sea state stands for a short period. This result was also supported by Yang et al. (2019), who examined the prototype scale of a WEC-DMDS. According to their result, for an energy wave period,  $T_e$ , of less than 3 s (classified in local wind seas), the efficiency was below 5%, which is even lower until 0%. This happens for the following reason: because of a short-wave period, the lever movement is not in an optimal position; thus, the buoy produces a shorter amplitude in the heave motion. If this amplitude is converted into rotational motion, it yields a short rotation, which is not sufficient to rotate the generator. In addition, this phenomenon can occur under sea-state conditions that have high wave steepness; thus, this problem needs to be further investigated. To address this problem, designing a mechanical system as effectively as possible is an optimal solution. Therefore, this study focuses on an oscillating buoy WEC based on a DMDS concept called the unidirectional cascaded gear wave energy converter (UCG-WEC). This design aims to address the drawbacks of a DMDS-WEC when applied in a short-wave period. This design is realized using a cascaded gear system and flywheel that can work when the wave goes up and down to produce a suitable rotation from a short heave motion.

## 2. Methods

This study aims to experimentally investigate the UCG-WEC performance in a short-wave period. The chosen short-wave period was obtained from the previous data of a WEC-DMDS prototype developed by Yang et al. (2019), which does not produce electricity at  $T_e < 3$  s. It is convenient to convert  $T_e$  to a regular wave period ( $T$ ) because this experiment uses a regular wave input. The equivalent value of  $T$  is defined as  $T_e = \alpha T_p = 0.946\alpha T$ , where  $\alpha$  is assumed to be equal to 1 (Hagerman, 2001). Thus, the  $T$  value is set to less than 2.84 s. The general procedure involves designing the UCG-WEC system, experimental setup, mounting preparation in a wave flume, and test definition.

### 2.1. UCG-WEC Design

A UCG-WEC is designed to extract wave energy based on the oscillating buoy concept. This device also uses the PTO mechanism based on a DMDS system. The mechanical system is designed such that optimal performance can be achieved. The complete design of the UCG-WEC system is illustrated in Figure 1a.

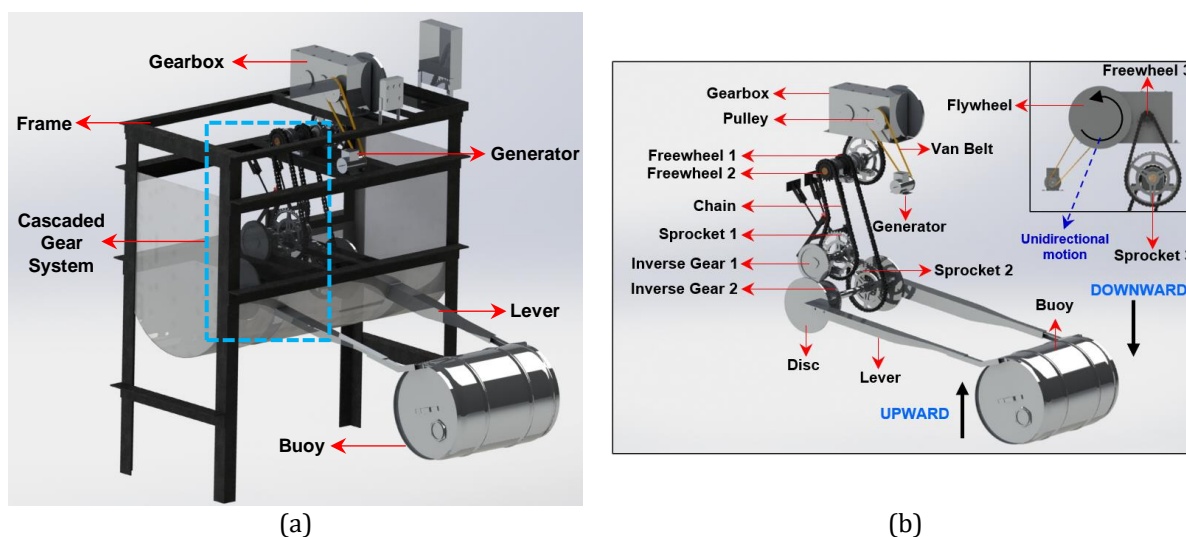


**Figure 1** (a) Design of the UCG-WEC system (b) and working mechanism of UCG-WEC

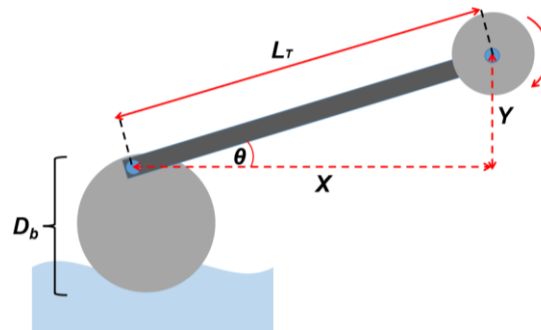
When an incoming wave reaches the UCG-WEC buoy, an upward and downward motion that is equivalent to the wave amplitude is formed along the z-axis direction. This motion drives a pair of levers to produce rotational motion. Because of the rotational motion, an angle change ( $\theta(t)$ ) occurs between the lever position and mean water level. This change produces unidirectional motion, which is launched by mechanical transmission in the form of a cascaded gear system. This system comprises components such as inverse gears, sprocket, freewheel, chain, and gearbox configuration to create unidirectional rotation and increase the small heave motion. Eventually, this unidirectional motion is transmitted to a pulley, which is linked to a generator shaft by a van belt. In addition, the flywheel enables a more continuous rotation system and stores the rotational energy to enhance the generator performance. By using the unidirectional rotation concept, the UCG-WEC can extract wave power optimally when it reaches the wave crest and the wave trough. The working of the UCG-WEC components under these conditions is shown in Figure 1b. The UCG-WEC is designed to harvest short-wave periods, which mostly occur in coastal areas where the local wind is the main cause of wave generation. The UCG-WEC can be integrated into a breakwater, a jetty, or other coastal structures. In addition, the UCG-WEC can be implemented by attaching it to offshore structures.

### 2.2. Experimental Setup

The study mainly aims to obtain increased UCG-WEC efficiency during a short-wave period. This was achieved by experimentally investigating the physical models of a UCG-WEC subjected to the test configurations listed in Table 1. These configurations comprise variations in the lever length and effective height, which are measured from the center of rotation of the lever to X, as depicted in Figure 2. By considering two physical variables, i.e., the lever length ( $L_T$ ) and effective height of the model to the water surface ( $Y$ ), the desired output can be achieved more accurately. The UCG-WEC is designed to work well in two-wave phases (when the wave goes up and down) with maximum power conversion.

**Table 1** Dimensions of UCG-WEC components

Component	Value
Frame dimensions	1 m x 0.5 m x 1.15 m
Lever length variation	0.9 m, 1.0 m, 1.15 m
Effective height variation	0.67 m and 0.37 m
Buoy dimensions	$D_b = 0.325$ m; $l_b = 0.45$ m
Flywheel dimensions	$D_f = 0.2$ m; $l_f = 0.007$ m
Transmission ratios I, II, III	1:2.44, 1:2.44, 1:10.56

**Figure 2** Experimental variable scheme**Table 2** Variations in the experiment

Configuration	Lever Length ( $L_r$ )	Effective Height ( $Y$ )	Relative Length Ratio ( $Y/L_r$ )
A	1.00 m	0.67 m	0.67
B	1.15 m	0.67 m	0.58
C	0.90 m	0.67 m	0.74
D	0.90 m	0.37 m	0.41
E	1.00 m	0.37 m	0.37
F	1.15 m	0.37 m	0.32

The UCG-WEC mechanical system modification focuses on the gear ratio and flywheel inertia. The wave motion moves the lever position by only about a quarter of a turn; thus, the gearbox is used to increase this rotation. The flywheel helps store energy so that the UCG-WEC can operate continuously. The UCG-WEC efficiency can be calculated from the electrical output power and captured power of the buoy.

### 2.3. Mounting Preparation in Flume Tank

The experiment was conducted in 2D flume tank facilities at Ocean Engineering, ITS Surabaya. The flume is 20.3 m long, 2.3 m wide, and 0.63 m deep. The flume tank is equipped with a wave absorber, a plunger-type wave generator, and regular-irregular wave generation features. In regular wave generation, the maximum wave height is 25 cm, with a wave period of approximately 0.5–3 s. It is also equipped with wave sensor probes connected to an analog-to-digital converter. This device transfers data to a computer set as a data recorder. An inertial measurement unit (IMU) sensor, a widely used motion measuring device, was employed to record the buoy motion (Pribadi & Shinoda, 2022). This peripheral consists of an accelerometer and a gyroscope combined in MPU 6050 GY 521 sensor, which is placed in the UCG-WEC lever. The MPU 6050 GY 521 sensor is connected to an inclining test software developed by LabView, which is previously installed in a computer. Also, this sensor is calibrated first and achieves a mean error of 1.94%, which indicates high accuracy. In addition, the power output of the UCG-WEC is measured by a data logger based on an INA219I2C sensor to obtain the voltage and current data of the generator. This device is calibrated and achieves a mean error of 4.6%.

This experiment uses only the front-wave probe to measure the input wave, which is located approximately 7 m from the wavemaker machine. Moreover, the distance between the front-wave probe and the buoy that has the longest lever variation is determined, with the aim of reducing the wave reflection when a wave hits the buoy. This phenomenon can affect the readout of wave probes, if not anticipated correctly. This distance is determined by referring to Goda and Suzuki (1976) and Isaacson (1991). It can be expressed as  $\delta l = 2L_{max}$ , where  $L_{max}$  is the longest wavelength produced by the highest selected test periods of 0.8, 1, and 1.2 s. The value of  $L$  is calculated using the wavelength equation for deep water by using Equation (1). As a result, the  $L_{max}$  value is approximately 4.5 m, as shown in the model mounting in Figure 3.

$$L = \frac{gT^2}{2\pi} \tag{1}$$

### 2.4. Test Definition

The main parameters scaled in the experimental study are the buoy dimension and test wave. The scale ratio for the model is selected as 1:3.7 by referring to the WEC experiment conducted by Yang et al. (2019) with the same values of diameter, width, and mass, as shown in Table 4. Also, the flywheel inertia of the WEC by Yang et al. (2019) is 100 kg.m<sup>2</sup>; thus, it is designed with lighter inertia and a ratio of 1:17. The wave periods of 1.4, 1.8, and 2.2 s are selected, which correspond to a short-wave period limit of  $T < 2.84$  s. These periods have scaled results of 0.8, 1, and 1.2 s, respectively. The scaled wave heights are 0.45, 0.5, and 0.55 m. According to the experimental results, the recorded wave periods are 0.75, 0.93, and 1.12 s, and the recorded wave heights are 0.12, 0.135, and 0.145 m.

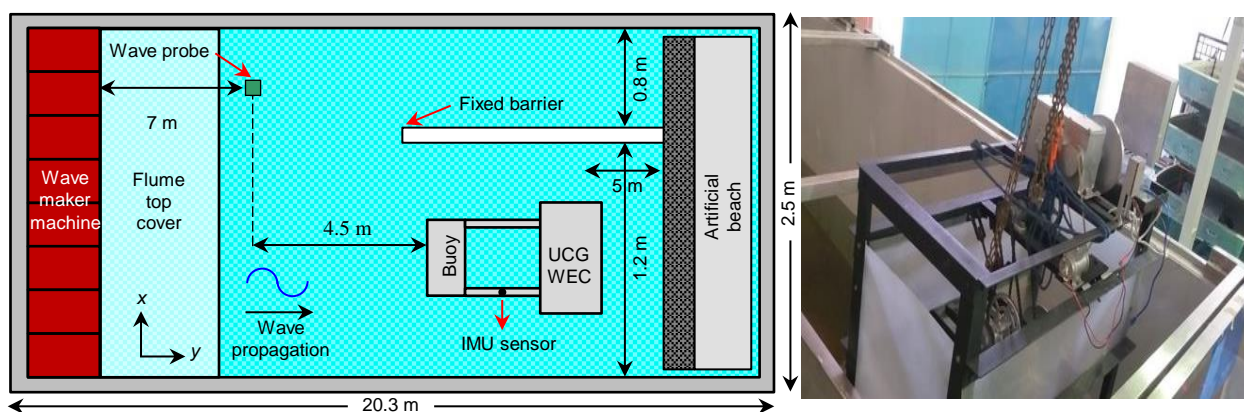


**Figure 3** Model mounting configuration on the flume tank

**Table 4** Scaling results with a scale factor (SF) of 3.7 and test realization

Parameters	SF	Prototype Scale	Model Scale	Experimental Result
Buoy mass ( $m_b$ )	$\lambda^3$	200 kg	3.948 kg	3.815 kg
Buoy diameter ( $D_b$ )	$\lambda$	1.2 m	0.324 m	0.325 m
Buoy width ( $B_b$ )	$\lambda$	1.7 m	0.46 m	0.45 m
Inertia flywheel ( $J_f$ )	$\lambda^5$	6 kg.m <sup>2</sup>	0.00865 kg.m <sup>2</sup>	0.0866 kg.m <sup>2</sup>
Wave period ( $T$ )	$\lambda^{1/2}$	1.4 s, 1.8 s, 2.2 s	0.8 s, 1 s, 1.2 s	0.75 s, 0.93 s, 1.12 s
Wave height ( $H$ )	$\lambda$	0.45 m, 0.5 m, 0.55 m	0.12 m, 0.135 m, 0.145 m	0.122 m, 0.135 m, 0.144 m

The wave parameters for the prototype scale are determined by considering the sea wave conditions in Indonesia. According to the results of the spatial variability analysis conducted in the global wave climate by Fairley et al. (2020), the Indonesian archipelago is classified as an enclosed sea, where the average significant wave height in the Indonesian sea was calculated as less than 1 m by Vettor and Soares (2020). Based on the Douglas Sea

Scale, which is largely adopted in the Sea State Code by the World Meteorological Organization (WMO), oceans with significant wave heights between 0.5 and 1.25 m fall into the slight sea-state category.

2.5. Data Measurement and Processing Method

The output data in this study are presented in the form of voltage ( $V_o$ ) and current ( $I_o$ ) data. Therefore, the electrical power output ( $P_e$ ) can be calculated using Equation (2).

$$P_e = V_o \cdot I_o \tag{2}$$

In addition, the power efficiency in the primary stage is determined based on the CWR. CWR represents hydrodynamic performance which mainly considered not only for WEC but also in other technology such as turbine (Soesanto et al., 2019) and ship (Paroka et al., 2021). CWR shows the power flow efficiency for each stage, which involves the efficiencies of the buoy ( $\eta_b$ ), mechanical system ( $\eta_m$ ), and generator ( $\eta_g$ ) as shown in Equation (3).

$$CWR = \frac{P_e}{P_c} = \eta_b \cdot \eta_m \cdot \eta_g \tag{3}$$

where  $P_e$  is given by Eq. (2) and  $P_c$  is the captured potential power (W) formulated by Equation (4) as follows

$$P_c = \frac{\rho g^2}{32\pi} H^2 T B_b \tag{4}$$

whre  $\rho$  is the water density ( $\text{kg/m}^3$ ),  $g$  is the gravitational acceleration ( $\text{m/s}^2$ ),  $H$  is the wave height (m),  $T$  is the wave period (s), and  $B_b$  is the buoy width (m).

3. Results and Discussion

3.1. Effect of Wave Period on Output Power

Figures 4(a) and 4(b) show the output power obtained from the changes in the incident wave period, which are tested at wave heights of 0.12, 0.135, and 0.145 m, respectively. As the wave period increases, the power gradually increases. This is because the buoy can move with a longer deviation due to the adequate time available to reach the maximum amplitude.

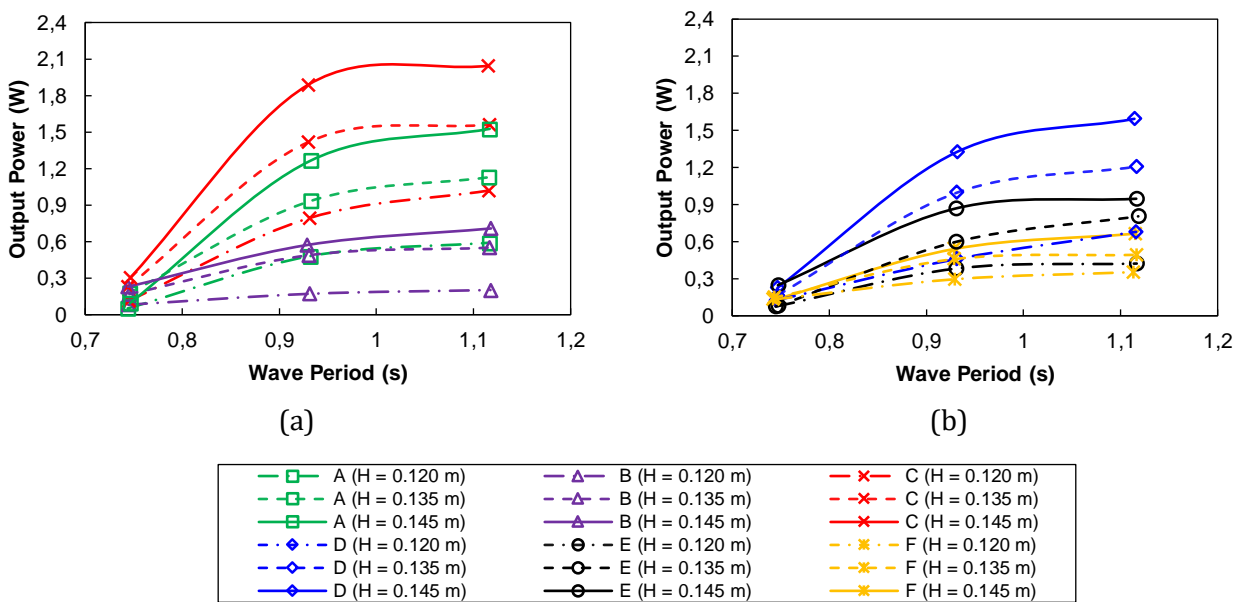
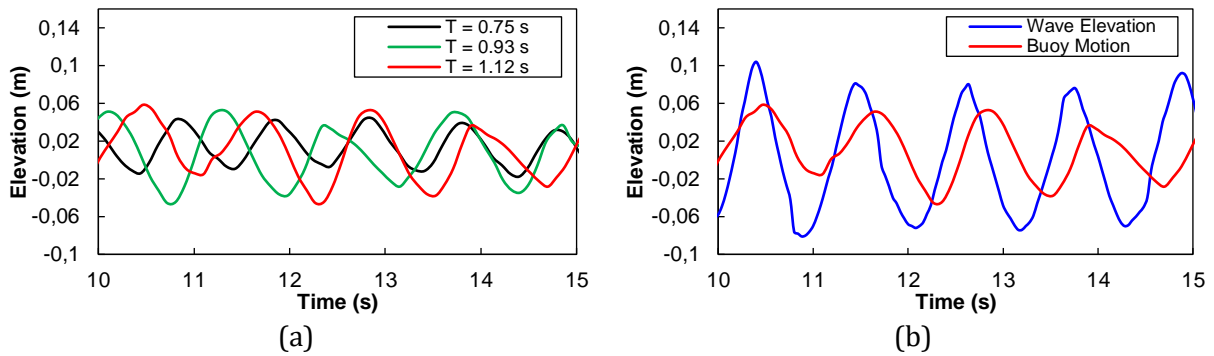


Figure 4 (a) Output power of A, B, C; and (b) D, E, F configurations in a short-wave period for all H variations



**Figure 5** (a) Buoy displacement comparison in all testing periods at  $H$  of 0.145 m. (b) Wave elevation and buoy motion characteristics at  $H$  of 0.145 m and  $T$  of 1.12 s

In a shorter period, the buoy oscillation tends to be fast and, thus, it cannot reach its maximum amplitude. These responses are also affected by the hydrodynamic coefficient in terms of added mass, damping, and restoring coefficients. The use of cascaded gear and lighter flywheels helps to convert small amplitudes into high rotations, thus helping the generator produce electricity. It is also seen that power increases with wave height. The resulting graph should be completely linear because the power is directly proportional to the wave height and wave period. However, in the wave period ranging between 0.93 and 1.12 s, the power values tend to be constant. This indicates that the UCG-WEC has reached its optimal working point and possibly produces steady power over a longer period. This analysis result is validated by the fact that the buoy heaving motion in these wave periods has a close amplitude, as shown in Figure 5a. This condition occurs because the UCG-WEC mechanical system is specially designed for a short-wave period in which the maximum deviation of buoy motion due to the wave is equivalent to a  $5^\circ$  effective revolution of the gear. For all configurations, the highest power occurs at a wave height of 0.145 m during the same wave period. The C configuration produces much higher power than the other configurations when the wave periods are longer than 0.8 s. However, this configuration cannot achieve maximum power because the buoy does not operate at resonance. As shown in Figure 5b, the buoy heaving elevation has a phase lag of approximately  $90^\circ$ , and its displacement is smaller than the wave amplitude. This phase lag indicates that when the wave begins to propagate, the buoy is still at rest and moves a few moments after the wave hits the buoy. In general, the UCG-WEC works properly to produce a certain amount of power in the short-wave period, especially for  $T < 2.84$  s in an actual application.

### 3.2. Effect of Relative Length Ratio

The heave amplitude of the UCG-WEC buoy depends on the relative length ratio ( $Y/L_T$ ). This parameter represents the ratio between the effective height and lever length, as shown in Table 2. Figure 6a shows that the highest power generated in the C configuration has a  $Y/L_T$  of 0.74. Note that a larger relative length ratio does not always produce considerable power. Evidently, the D variation has a higher power than A and B; thus, the UCG-WEC works at the most optimal relative length ratio. This parameter affects the rotational angle acting on the lever, as shown in Figure 6b. The  $\theta$  value of  $31.86^\circ$  is the optimal angle because it is obtained from the  $Y/L_T$  value of 0.74, which is the most optimal configuration. At the same value of  $L_T$ , the highest power occurs at each  $Y$  value of 0.67 m; thus, the configurations are in the following order:  $C > D$ ,  $A > E$ , and  $B > F$ . In addition, C and D can produce the highest power because they have the shortest lever at the same effective height. The shortest lever can produce faster angular acceleration, thereby increasing the flywheel torque value. The higher the flywheel torque value, the higher is the total power generated.

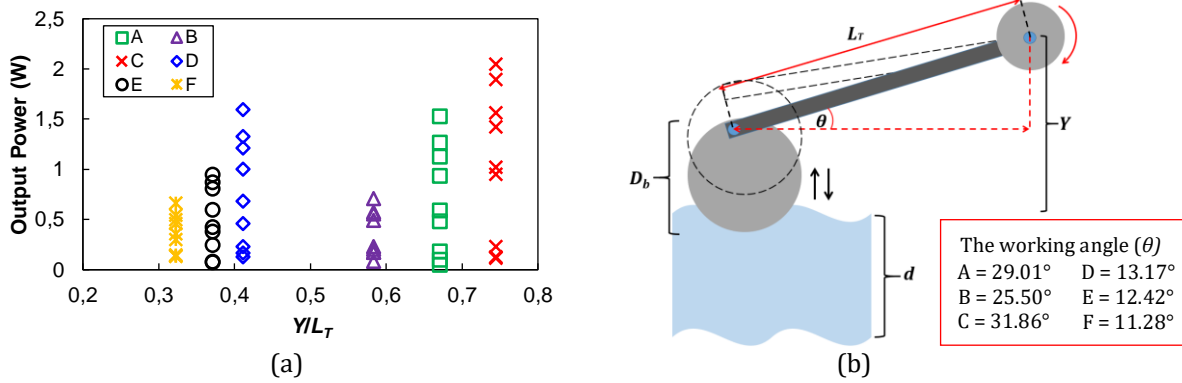


**Figure 6** (a) Effect of  $Y/L_T$  on the output power in all test waves. (b) Illustration of buoy movement and its working angle in all configurations

3.3. CWR and UCG-WEC Mechanical Efficiency

In this study, the performance of UCG-WEC is assessed based on the CWR value, which represents the hydrodynamic efficiency of the system. To be more realistic, the CWR values obtained from the experimental results are converted to a prototype scale using the similarity law. As shown in Figures 7a and 7b, the highest CWR and output power in all configurations are concentrated at a wave steepness of 0.012. This steepness value is calculated from the highest wave height and longest wave period. By applying the fixed buoy width, the CWR characteristic is slightly different from the output power because it is affected by different potential captured power ( $P_c$ ). Since  $H$  and  $T$  are directly proportional to  $P_c$ , the power absorption probability is increased so that the CWR value can be made more efficient. The C configuration evidently has the highest CWR and power; thus, the next analysis will focus on this type only.

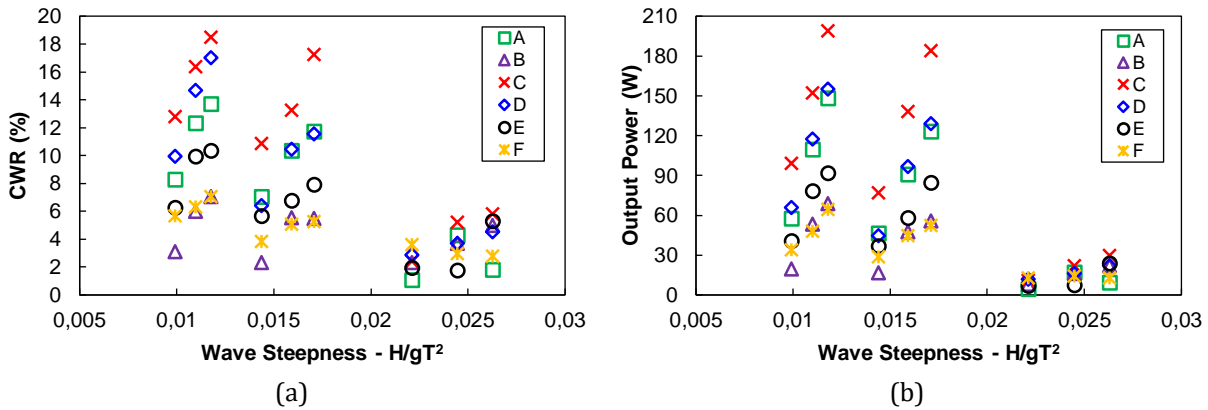


**Figure 7** (a) Characteristic of CWR and (b) output power to the wave steepness

In the sea-state variation, the maximum CWR of 18.5% occurs at  $H$  of 0.55 m and  $T$  of 2.2 s, as shown in Figure 8a. This CWR value can provide an output power of 200 W and mechanical efficiency of up to 87%, as shown in Figures 8b and 8c, respectively. The UCG-WEC clearly performs better than the model proposed by Yang et al. (2019) in a short-wave period. In addition, the CWR value is easier to analyze using the power flow concept. This concept begins with the conversion of  $P_c$  into the absorbed power of the buoy ( $P_b$ ), mechanical power ( $P_m$ ), and electrical power ( $P_e$ ). As shown in Figure 8d, the efficiency of  $P_b$  is smaller than that of  $P_c$ , but it is converted maximally become  $P_m$  and  $P_e$  in the next conversion. The minimum mechanical power loss of the UCG-WEC is still approximately 13%. This limitation is affected by factors such as the “spelling” behavior of the freewheel, mechanical friction, and the nonlinear interaction among the cascaded gear components. The “spelling” phenomenon occurs because the freewheel uses some energy to create an

initial rotation of its internal bullet. When the buoy moves at a certain deviation, the freewheel uses this motion to start rotating; thus, the initial rotation of the gearbox comes from the effective displacement of the second mechanical transmission stage.

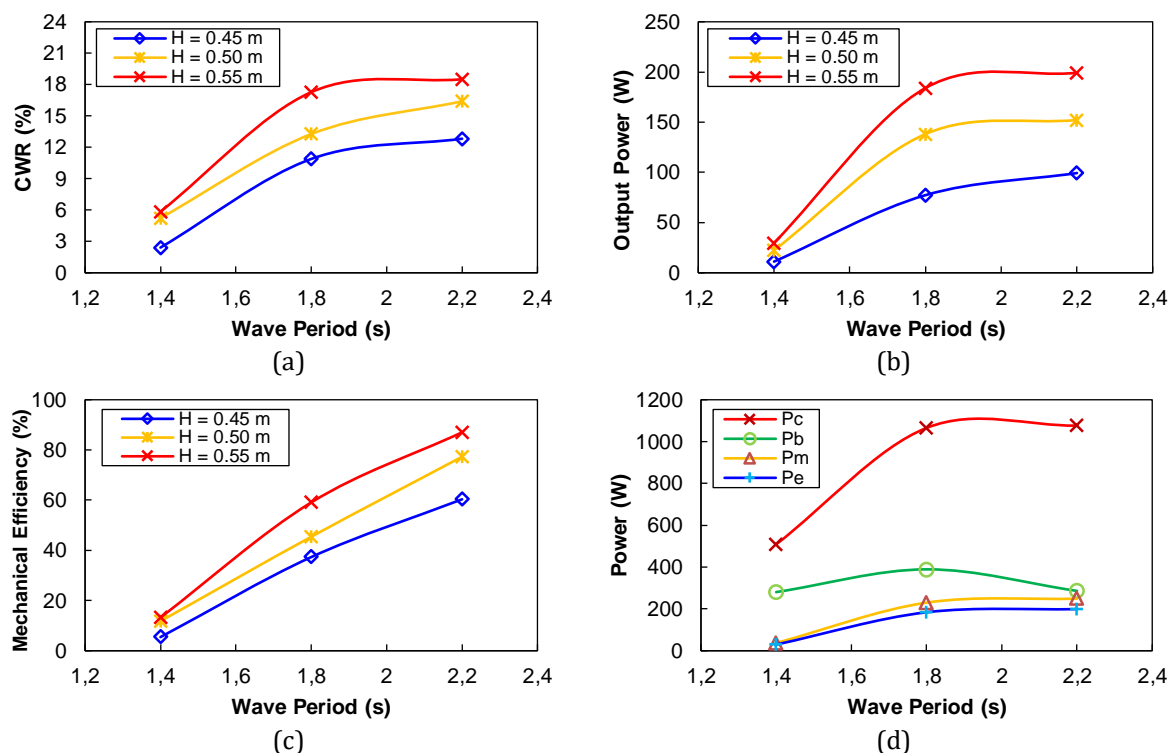


**Figure 8** (a) CWR, (b) output power, (c) mechanical efficiency, (d) and power flow of C configuration in short-wave period under an actual condition

### 3.4. Comparison with the Other DMDS System

To analyze the performance of the UCG-WEC mechanical system, it is compared with similar DMDS-WEC models. Some of the compared models are listed in Table 5, and the results are shown in Figure 9. To obtain the mechanical efficiency from the references, a calculation process is performed using Eq. (3), where the mechanical power ( $P_m$ ) is divided by the power absorption of the buoy ( $P_b$ ). Not all previous studies included the  $P_b$  values; thus, it needs to be calculated through the assumption of buoy efficiency based on the geometric shape determined by Shi et al. (2019). According to the comparison results, the previous models focused on low wave steepness. At wave steepness below 0.012, the UCG-WEC exhibits higher mechanical efficiency than the other five models and only 6% lower efficiency difference as compared to Chandrasekaran and Harender’s (2012) model. Meanwhile, at a higher wave steepness of up to 0.026, the UCG-WEC mechanical system has 13% efficiency, which is 4% higher than that of Peng et al.’s (2015) model. This comparison indicates that the UCG-WEC works well under both high-and low-wave steepness conditions.

**Table 5** DMDS mechanism configurations in previous studies

Authors	DMDS System	Selected $H/gT^2$ range
Lok (2010)	Gear-flywheel system	0.00108–0.00843
Chandrasekaran & Harender (2012)	Rack and chain-gear system	0.00113–0.00453
Chandrasekaran & Raghavi (2015)	Lever and gear-flywheel system	0.00272–0.00340
Han et al. (2015)	Counterweight and flywheel system	0.00255–0.01258
Peng et al. (2015)	Rack-cascaded gear and flywheel system	0.02000–0.04000
Binh et al. (2016)	Rack gear and flywheel system	0.00214–0.00301
Present	Lever and cascaded gear-flywheel system	0.00991–0.02628

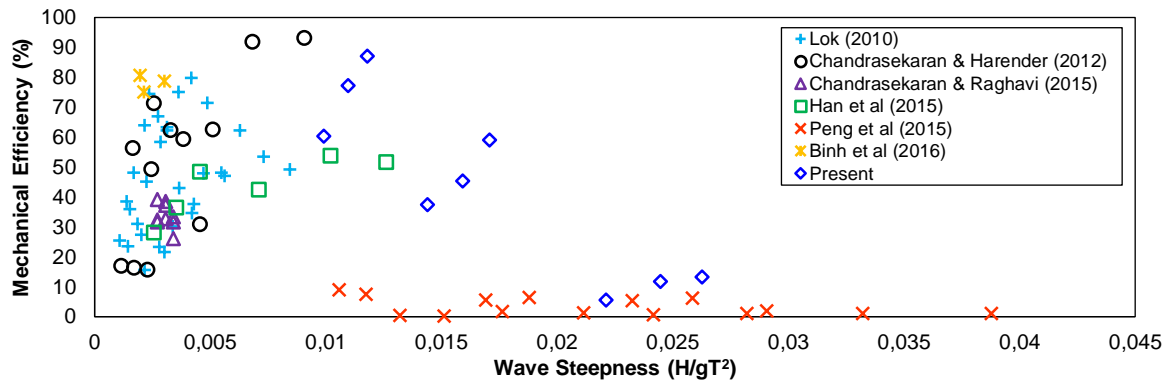


**Figure 9** Comparison of CWR with those obtained in previous DMDS studies

#### 4. Conclusions

According to the experimental results, the UCG-WEC can work appropriately in a short-wave period, especially for  $T < 2.84$  s. The maximum efficiency of the UCG-WEC is approximately 18.5% for CWR and 87% for mechanical efficiency. These efficiencies lead to a maximum power of 200 W for actual conditions. This result is achieved in the C configuration, which has a relative length ratio of 0.74. This study shows that modifying the DMDS configuration can increase the efficiency of a WEC for a sea state that has certain limitations. Compared to the previous experiment, the UCG-WEC can produce considerable energy under short-wave conditions, and its efficiency can be increased. In addition, the UCG-WEC performs well under both high-and low-wave steepness conditions.

#### Acknowledgements

The authors express their gratitude to the Ministry of Education and Culture of Indonesia and Lembaga Pengelola Dana Pendidikan (LPDP) for providing the research grant and college opportunity. This research was also supported by the Laboratory of Energy and Coastal Environment, Department of Ocean Engineering, Institut Teknologi Sepuluh Nopember (ITS), Indonesia.

#### References

- Ahn, S., Haas, K.A., Neary, V.S., 2019. Wave Energy Resource Classification System for US Coastal Waters. *Renewable and Sustainable Energy Reviews*, Volume 104, pp. 54–68
- Binh, P.C., Tri, N.M., Dung, D.T., Ahn, K.K., Kim, S.J., Koo, W., 2016. Analysis, Design, and Experiment Investigation of a Novel Wave Energy Converter. *IET Generation, Transmission & Distribution*, Volume 10(2), pp. 1–10
- Chandrasekaran, S., Harender., 2012. Power Generation Using Mechanical Wave Energy Converter. *International Journal of Ocean and Climate Systems*, Volume 3(1), pp. 57–70
- Chandrasekaran, S., Raghavi, B., 2015. Design, Development and Experimentation of Deep Ocean Wave Energy Converter System. *Energy Procedia*, Volume 79, pp. 634–640
- Chen, F., Duan, D., Han, Q., Yang, X., Zhao, F., 2019. Study on Force and Wave Energy Conversion Efficiency of Buoys in Low Wave Energy Density Seas. *Energy Conversion and Management*, Volume 182, pp. 191–200
- Fairley, I., Lewis, M., Robertson, B., Hemer, M., Masters, I., Caraballo, J.H., Karunarathna, H., Reeve, D.E., 2020. A Classification System for Global Wave Energy Resources Based on Multivariate Clustering. *Applied Energy*, Volume 262, pp. 1 – 21
- Falcão, A.F., 2010. Wave Energy Utilization: A Review of the Technologies. *Renewable and Sustainable Energy Reviews*, Volume 14(3), pp. 899–918

- Farrok, O., Ahmed, K., Tahlil, A.D., Farah, M.M., Kiran, M.R., Islam, M.R., 2020. Electrical Power Generation from the Oceanic Wave for Sustainable Advancement in Renewable Energy Technologies. *Sustainability*, Volume 12(6), p. 2178
- Goda, Y., Suzuki, Y., 1976. Estimation of Incident and Reflected Waves in Random Wave Experiments. *Coastal Engineering Proceedings*, Volume 1(15), p. 47
- Hagerman, G., 2001. Southern England Wave Energy Resource Potential. *In: Proceedings of Building Energy 2001*, Boston, Massachusetts, USA
- Han, S.H., Jo, H.J., Lee, S.J., Hwang, J.H., Park, J.W., 2015. Experimental Study on Performance of Wave Energy Converter System with Counterweight. *Journal of Ocean Engineering and Technology*, Volume 30(1), pp. 1–9
- Isaacson, M., 1991. Measurement of Regular Wave Reflection. *Journal of Waterway, Port, Coastal and Ocean Engineering*, Volume 117(6), pp. 553–569
- Li, D., Li, D., Li, F., Shi, J., Zhang, W., 2013. Analysis of Floating Buoy of a Wave Power Generating Jack-Up Platform Haiyuan 1. *Advances in Mech Engineering*, Volume 5, pp. 1–7
- Lok, K.S.K., 2010. *Optimization of the Output of a Heaving Wave Energy Converter*. Master's Thesis, Graduate Program, Faculty of Engineering and Physical Science, University of Manchester, UK
- López, I., Andreu, J., Ceballos, S., Martínez De Alegría, I., Kortabarria, I., 2013. Review of Wave Energy Technologies and the Necessary Power-Equipment. *Renewable and Sustainable Energy Reviews*, Volume 27, pp. 413–434
- Mueller, M.A., Baker, N.J., 2005. Drive Electrical PTO for Offshore Marine Energy Converters. *In: Proceedings of the Institution of Mechanical Engineers, Part A: Journal of Power and Energy*, Volume 219, pp. 223–234
- Peng, W., Lee, K.H., Mizutani, N., Huang, X., 2015. Experimental and Numerical Study on Hydrodynamic Performance of a Wave Energy Converter Using Wave-Induced Motion of Floating Body. *Journal of Renewable and Sustainable Energy*, Volume 7(5), pp. 1–29
- Rahmati, M.T., Aggidis, G.A., 2016. Numerical and Experimental Analysis of the Power Output of a Point Absorber Wave Energy Converter in Irregular Waves. *Ocean Engineering*, Volume 111, pp. 483–492
- Paroka, D., Muhammad, A.H., Rahman, S. 2021. Hydrodynamics Factors Correspond to the Weather Criterion Applied to an Indonesian Ro-Ro Ferry with Different Weight Distributions. *International Journal of Technology*, Volume 12(1), pp. 126–138
- Pribadi, T.W., Shinoda, T. 2022. Hand Motion Analysis for Recognition of Qualified and Unqualified Welders using 9-DOF IMU Sensors and Support Vector Machine (SVM) Approach. *International Journal of Technology*, Volume 13(1), pp. 38–47
- Shi, H., Huang, S., Cao, F., 2019. Hydrodynamic Performance and Power Absorption of a Multi Freedom Buoy Wave Energy Device. *Ocean Engineering*, Volume 172, pp. 541–549
- Soesanto, Q.M.B., Widiyanto, P., Susatyo, A., Yazid, E. 2019. Cascade Optimization of an Axial-Flow Hydraulic Turbine Type Propeller by a Genetic Algorithm. *International Journal of Technology*, Volume 10(1), pp. 200–211
- Têtu, A., 2017. *Handbook of Ocean Wave Energy*. In: Pecher, A., (ed.), SpringerOpen, Bern, p. 213
- Vettor, R., Soares, C.G., 2020. A Global View on Bimodal Wave Spectra and Crossing Seas from ERA-Interim. *Ocean Engineering*, Volume 210, pp 1–13
- Yang, S., He, H., Chen, H., Wang, Y., Li, H., Zheng, S., 2019. Experimental Study on the Performance of a Floating Array-Point-Raft Wave Energy Converter Under Random Wave Conditions. *Renewable Energy*, Volume 139, pp. 538–550